AN EMPIRICAL EQUATION FOR PREDICTING PAVEMENT DEFLECTIONS

By

F. H. Scrivner
Research Engineer

W.M. Moore
Associate Research Engineer

Research Report 32-12

Extension of
AASHO Road Test Results
Research Study Number 2-8-62-32

Sponsored By

The Texas Highway Department
In Cooperation with the
U. S. Department of Transportation
Federal Highway Administration
Bureau of Public Roads

October, 1968

TEXAS TRANSPORTATION INSTITUTE
Texas A&M University
College Station, Texas

TABLE OF CONTENTS

LIST OF TABLES

LIST OF FIGURES

ACKNOWLEDGEMENTS

The authors appreciate the constribution to this report of Dr. H. O. Hartley of Texas A&M University, who furnished the experiment design for the construction of the pavement test facility; and of District Engineer C. B. Thames of the Texas Highway Department, whose maintenance forces constructed the test facility.

The opinions, findings, and conclusions expressed in this publication are those of the authors and not necessarily those of the Bureau of Public Roads.

1. INTRODUCTION

This report is intended to document the empirical equation for predicting pavement deflections given in Section 3.2 of Research Report 32-11, "A Systems Approach to the Flexible Pavement Design Problem"(1). The equation predicts deflections measured by the Dynaflect*, given certain design parameters for the pavement.

The equation was derived in two basic steps: (1) a mathematical model of the deflection phenomenon, containing certain undetermined coefficients, was developed, and (2) the coefficients were evaluated by fitting the model to Dynaflect deflection data gathered on a set of special test sections constructed in accordance with statistical principles of experiment design. This report presents the model, describes how the coefficients were evaluated, discusses the prediction errors associated with the equation, and shows how the model can be used to estimate stiffness coefficients in simple pavement structures.

How the equation is used to solve practical problems of design is described briefly in a summary report, "The Design of Flexible Pavements (A Systems Approach)," and in detail in Research Report 32-11 (1).

---

*Registered Trademark, Dresser-Atlas Company, Dallas, Texas .

2. DEFLECTION MEASURING EQUIPMENT

In March, 1966, following the completion of Texas Transportation Institute's Pavement Test Facility described in Chapter 4, deflections were measured on the facility by means of the Dynaflect. Descriptions of the Dynaflect and examples of its use in pavement research have been published previously (1)(2)(3). Suffice it to say here that a dynamic load of 1000 lbs, oscillating sinusoidally with time at 8 cps, is applied through two steel load wheels to the pavement, as indicated in Figure 1. Five sensors, resting on the pavement at the numbered points shown in the figure, register the vertical amplitude of the motion at those points in thousandths of an inch (or mils).

A deflection basin of the type illustrated in Figure 2 results from the Dynaflect loading. The symbol W_1 represents the amplitude--or deflection--occurring at Point 1, W_2 is the deflection at Point 2, etc.

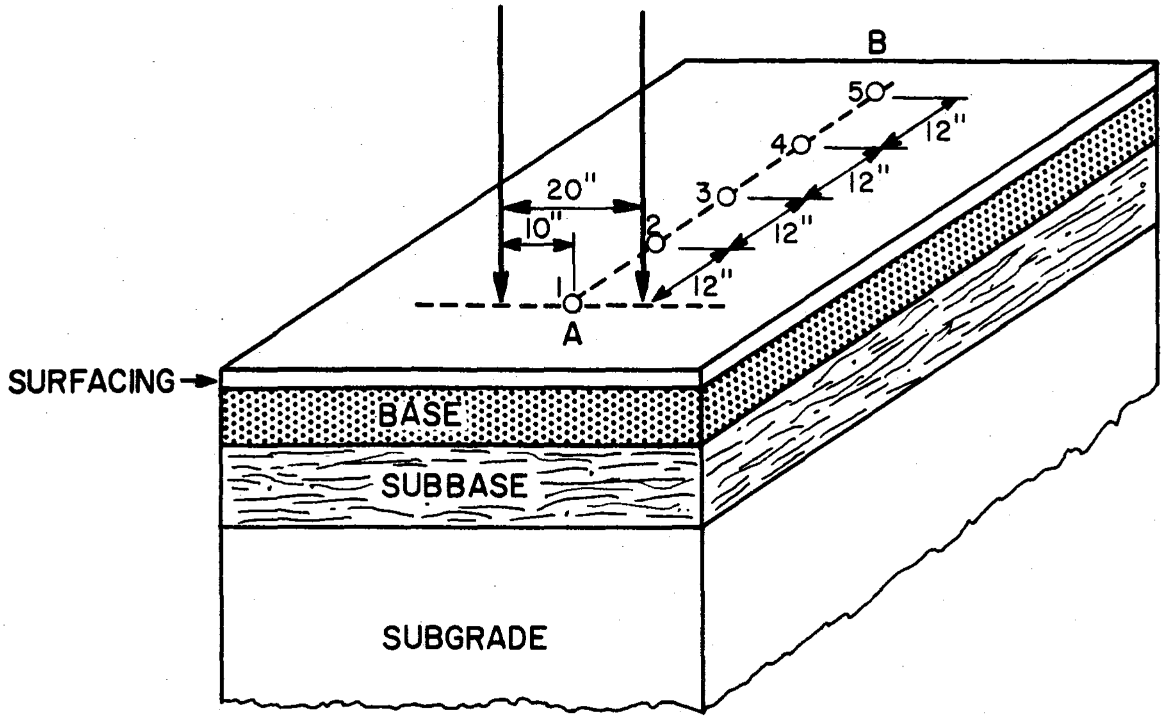

FIGURE 1: Position of Dynaflect sensors during test. Vertical arrows represent load wheels. Points numbered 1 through 5 indicate location of sensors.

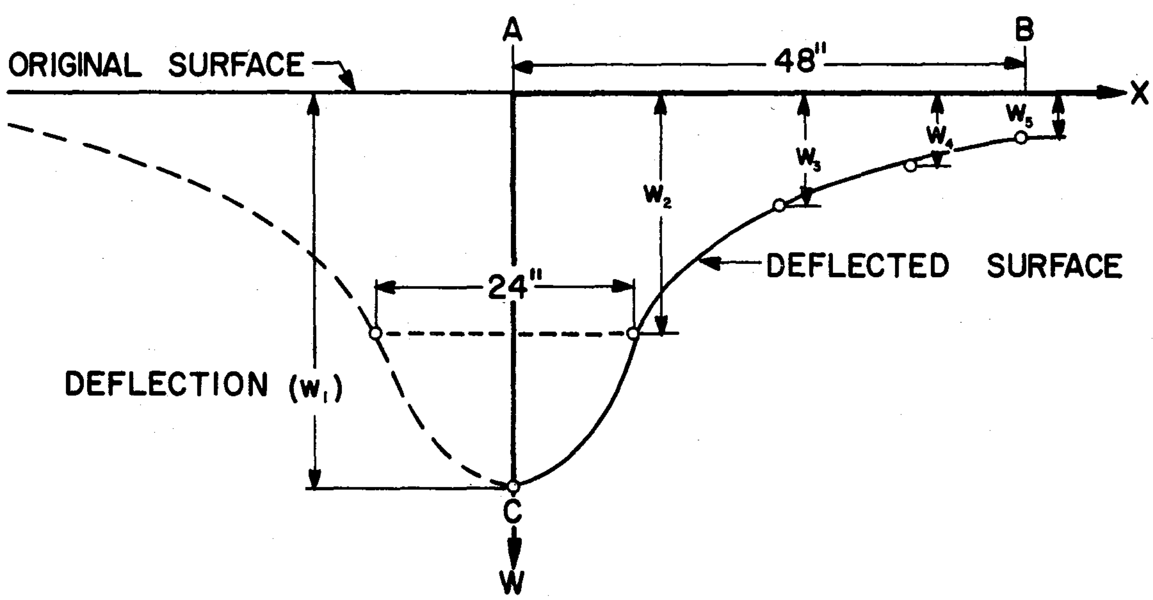

FIGURE 2: Typical deflection basin reconstructed from Dynaflect readings. Only half of basin is measured.

3. DESIGN VARIABLES

The sketch in Figure 3 represents a pavement composed of n layers above the subgrade level. The material in each of these layers, and in the foundation layer, is characterized by a strength coefficient, a_i, where the subscript, i, identifies the position of the layer in the structure. Layers are numbered consecutively from the top downward; thus, $i = 1$ for the surfacing layer, and $i = n + 1$ for the foundation layer, which is considered to be of infinite thickness. The thickness of any layer above the foundation is represented by the symbol, D_i.

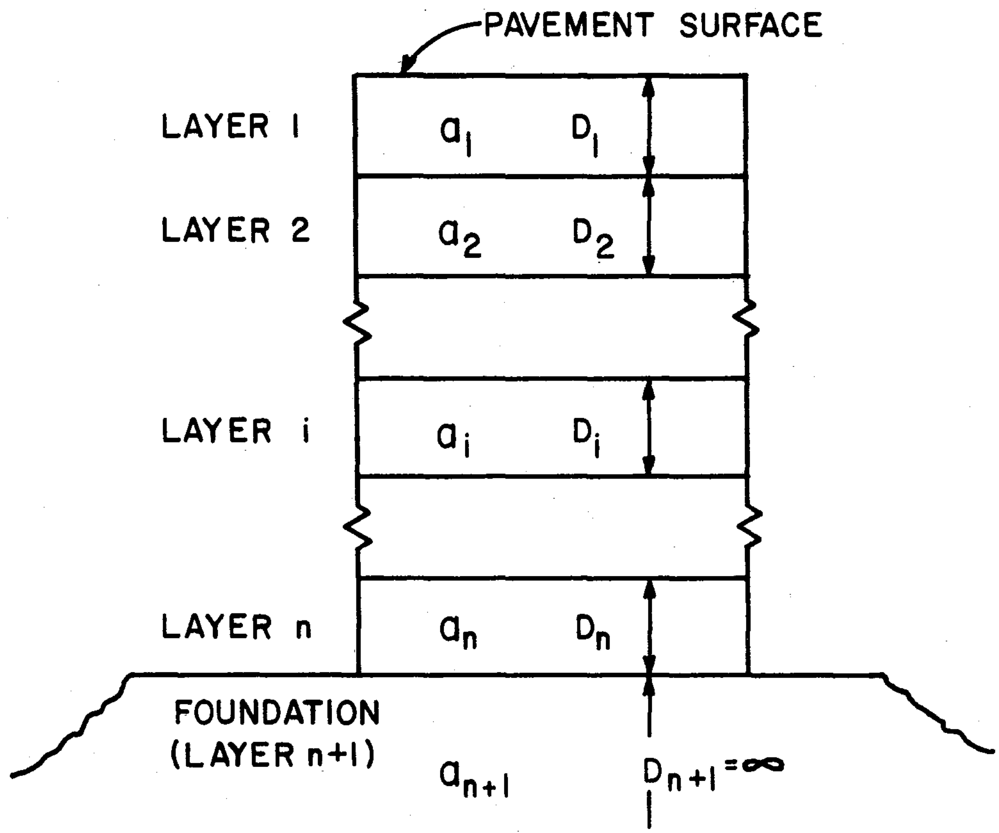

FIGURE 3: A pavement section of n layers above the subgrade level.

4. TEST FACILITY DESIGN VARIABLES AND DEFLECTION DATA

The A&M Pavement Test Facility, located at the University's Research Annex, was constructed for the sole purpose of providing a means for evaluating nondestructive testing techniques, or more particularly, for evaluating testing equipment purporting to furnish information concerning the in situ strength of individual layers in a flexible pavement. The design of the facility is described in detail in Reference 4. For present purposes it will suffice to say that it consists of 27 12- x 40-ft. test sections, desgined in accordance with the principles of statistical experiment design. The variables treated are indicated in tabular form in Table 1. The materials used are shown in Table 2 and the design variables for each section, as well as the measured deflection data, are given in Table 3.

Plan and cross-sectional views of the test facility are shown in Figures 4 and 5, respectively, and a photograph of the completed facility appears in Figure 6.

TABLE 1: LIST OF VARIABLES IN PAVEMENT TEST FACILITY

Variable	Levels: Low	Medium	High
Surface Thickness	1"	3"	5"
Base Thickness	4"	8"	12"
Subbase Thickness	4"	8"	12"
Base Material Type	4	5	6
Subbase Material Type	4	5	6
Embankment Material Type	1	2	3

TABLE 2: MATERIALS USED IN PAVEMENT TEST FACILITY

Material Type	Symbol for Stiffness Coefficient	Description	Where Used	AASHO Class.	Unified Soil Class.	Texas Triaxial Class.	Compressive Strength* psi	In Situ Wave Velocity ft./sec.
0	b_o	Plastic Clay	Foundation	A-7-6(20)	CH	--	--	--
1	b_1	Plastic Clay	Embankment	A-7-6(20)	CH	5.0	22	2412
2	b_2	Sandy Clay	Embankment	A-2-6(1)	SC	4.0	40	2576
3	b_3	Sandy Gravel	Embankment	A-1-6	SW	3.6	43	3721
4	b_4	Cr. Limestone	Base & Subb.	A-1-a	GW-GM	1.7	165	5222
5	b_5	Cr. Limestone + 2% Lime	Base & Subb.	A-1-a	GW-GM	--	430	5448
6	b_6	Cr. Limestone +4% Cement	Base & Subb	A-1-a	GW-GM	--	2270	7309
7	b_7	Asph. Concr.	Surfacing	--	--	--	--	--

*By Texas triaxial procedure, at a lateral pressure of 5 psi.

TABLE 3: DESIGN VARIABLES BY SECTION AND LAYER, AND DEFLECTION DATA

	Thickness (In.)*				Material Coefficients					Deflection Data				
	Surf.	Base	Subbase	Embank.										
Sec.	D_1	D_2	D_3	D_4	a_1	a_2	a_3	a_4	a_5	W_1	W_2	W_3	W_4	W_5
1	[illegible]	4	4	40	b_7	b_6	b_4	b_1	b_0	1.92	1.49	1.01	.60	[illegible]
2	1	12	4	36	b_7	b_6	b_4	b_1	[illegible]	.52	.47	.41	.34	
3	1	4	12	36	b_7	b_6	b_4	[illegible]	[illegible]	1.05	.86	.58	.39	
4	5	12	12	24	b_7	b_6	b_4	b_1	b_0	.37	.35	.32	.28	
5	5	4	4	40	b_7	b_4	b_6	b_1	b_0	1.26	.95	.61	.40	
6	1	12	4	36	b_7	b_4	b_6	b_1	b_0	1.16	[illegible]	.72	.49	
7	1	4	12	36	b_7	b_4	b_6	b_1	b_0	.74	[illegible]	.53	.42	.33
8	5	12	12	24	b_7	b_4	b_6	b_1	b_0	.62	[illegible]	.33	.28	.24
9	5	4	4	40	b_7			b_3	b_0	.75	[illegible]	.38	.27	.21
10	1	12	4	36	b_7	[illegible]	b_4	b_3	b_0	[illegible]	[illegible]	.40	.32	.26
11	1	4	12	36	b_7	b_4	b_4	b_3	b_0	.63	.48	.37	.28	.23
	5	12	12	24	b_7	b_4	b_4	b_3	b_0	.64	.45	.32	.25	.20
	5	4	4	40	b_7	b_6	b_6	b_3	b_0	.47	.43	.36	.28	.22
	1	12	4	36	b_7	b_6	b_6	b_3	b_0	.40	.37	.33	.27	.23
15	1	4	12	36	b_7	b_6	b_6	b_3	b_0	.41	.36	.32	.27	.22
16		12	12	24	b_7	b_6	b_6	b_3	[illegible]	.29	[illegible]	.25	.21	.19
17		8	8	34		[illegible]	b_5	b_2	[illegible]	.72	[illegible]	.44	.33	.26
18	1	8	8	36		[illegible]	b_5	b_2	[illegible]	.84	[illegible]	.48	.36	.28
19	5	8	8	32		[illegible]	[illegible]	[illegible]	[illegible]	.76	[illegible]	.48	.36	.28
20	3	4	8	38		[illegible]	[illegible]	[illegible]	[illegible]	.73	[illegible]	.47	.35	.27
21	3	12		30	b_7	b_5	[illegible]	b_2	[illegible]	.62	[illegible]	[illegible]	.33	.27
[illegible]	3	8	8	34	b_7	b_4	b_5	b_2	b_0	[illegible]		[illegible]	.34	.26
	3	8	8	34	b_7	b_6	b_5	b_2	b_0			[illegible]	[illegible]	[illegible]
			[illegible]	[illegible]				b_2	b_0					
				[illegible]				b_2	b_0					
				[illegible]				b_1	b_0					
				[illegible]				[illegible]	[illegible]	[illegible]	[illegible]			

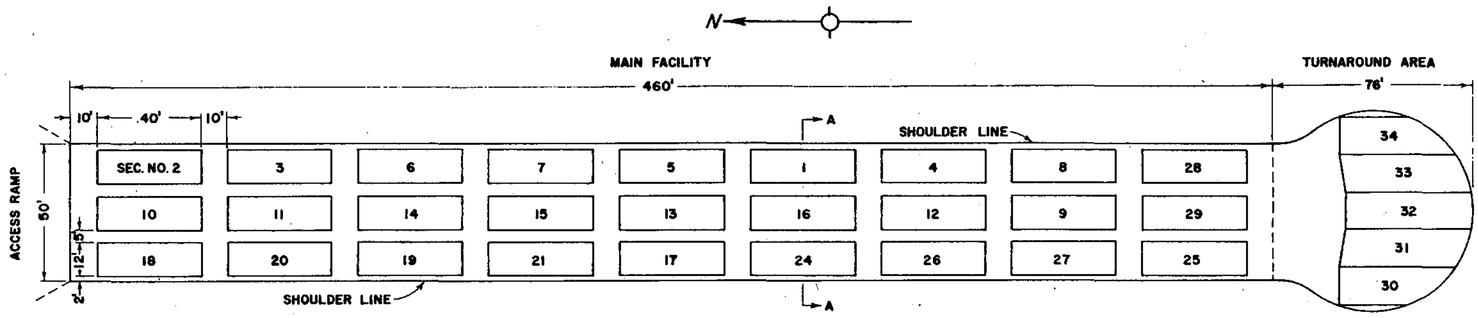

FIGURE 4: Plan view of pavement test facility.

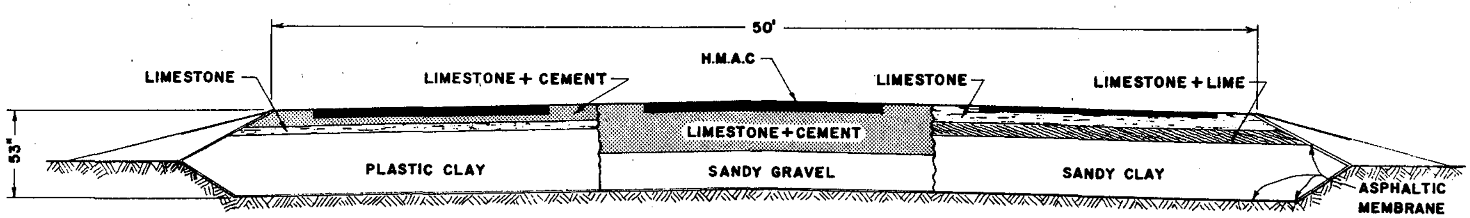

FIGURE 5: Cross-section of pavement test facility (Section A-A of Figure 4). Vertical distance from surface to foundation was held constant, thicknesses and materials between were varied as shown in Table 3.

FIGURE 6: View of completed facility.

5. THE DEFLECTION MODEL

A detailed discussion of the considerations leading to the particular form of the empirical mathematical model adopted to represent Dynaflect deflections is given in Appendix A. The model, selected after many exploratory analyses of the deflection data--including the analyses described in Research Reports 32-8 and 32-9--is given below.

$$W_j = \sum_{k=1}^{n+1} \Delta_{jk} \qquad (1)$$

where

$$\Delta_{jk} = \frac{C_o}{a_k^{C_1}} \left[\frac{1}{r_j^2 + C_2\left(\sum_{i=0}^{k-1} a_i D_i\right)^2} - \frac{1}{r_j^2 + C_2\left(\sum_{i=0}^{k} a_i D_i\right)^2} \right],$$

$a_o = D_o = 0$,

C_o, C_1, C_2 are constants,

r_j = the distance (inches) from point of application of either load to the j^{th} sensor ($r_1^2 = 100$, $r_2^2 = 244$, $r_3^2 = 676$, $r_4^2 = 1396$, $r_5^2 = 2404$), and the other variables, a_i and D_i, are as previously defined.

6. ANALYSIS OF DEFLECTION DATA

This chapter describes how the undetermined constants and stiffness coefficients in the model were evaluated from deflection data gathered on the test facility.

6.1 Objective of Analysis

The objective of the analysis procedure treated in this chapter was to find the particular set of values for the three constants C_o, C_1, C_2 and the eight stiffness coefficients, b_o, b_1, . . ., b_7, that would minimize the prediction error associated with Equation 1. Since the model is non-linear in the stiffness coefficients, finding the best set of values was not an easy and straight-forward task. As a result, the rather lengthy explanation that follows was necessary in order to document the procedure used.

6.2 Steps Preliminary to Regression A

We begin the description of the procedure followed in evaluating the eleven quantities listed above by writing Equation 1 in its extended form--that is, without summation signs--for a layered system with four layers (surface, base, subbase, embankment) above the foundation layer.

$$W_j = \Delta_{j1} + \Delta_{j2} + \Delta_{j3} + \Delta_{j4} + \Delta_{j5} \qquad (1a)$$

where

$$\Delta_{j1} = \frac{C_o}{a_1^{C1}} \left(\frac{1}{f_j^2} - \frac{1}{r_j^2 + C_2(a_1D_1)^2} \right),$$

$$\Delta_{j2} = \frac{C_o}{a_2^{C1}} \left(\frac{1}{f_j^2 + C_2(a_1D_1)^2} - \frac{1}{r_j^2 + C_2(a_1D_1 + a_2D_2)^2} \right),$$

$$\Delta_{j3} = \frac{C_o}{a_3^{C1}} \left(\frac{1}{f_j^2 + C_2(a_1D_1 + a_2D_2)^2} - \frac{1}{r_j^2 + C_2(a_1D_1+a_2D_2+a_3D_3)^2} \right),$$

$$\Delta_{j4} = \frac{C_o}{a_4^{C1}} \left(\frac{1}{f_j^2 + C_2(a_1D_1 + a_2D_2 + a_3D_3)^2} - \frac{1}{r_j^2 + C_2(a_1D_1 + a_2D_2 + a_3D_3 + a_4D_4)^2} \right), \text{ and}$$

$$\Delta_{j5} = \frac{C_o}{a_5^{C1}} \left(\frac{1}{r_j^2 + C_2(a_1D_1 + a_2D_2 + a_3D_3 + a_4D_4)^2} \right).$$

To illustrate how the extended equation can be used to write an equation for the deflection, W_j, in terms of the stiffness coefficients, b_i, for a given section, consider the data for Section 1 in Table 3. For this section: $D_1 = 5$, $a_1 = b_7$; $D_2 = 4$, $a_2 = b_6$; $D_3 = 4$, $a_3 = b_4$; $D_4 = 40$, $a_4 = b_1$; $D_5 = \infty$, $a_5 = b_o$. Let $j = 2$: then $r_j^2 = r_2^2 = 244$. With 5 substituted for D_1, b_7 for a_1, etc., in Equation 1a, we arrive at the following equation:

$$W_2 = B_7\left(\frac{1}{244} - \frac{1}{244 + C_2(5b_7)^2}\right)$$

$$+ B_6\left(\frac{1}{244 + C_2(5b_7)^2} - \frac{1}{244 + C_2(5b_7 + 4b_6)^2}\right)$$

$$+ B_4\left(\frac{1}{244 + C_2(5b_7 + 4b_6)^2} - \frac{1}{244 + C_2(5b_7 + 4b_6 + 4b_4)^2}\right)$$

$$+ B_1\left(\frac{1}{244 + C_2(5b_7 + 4b_6 + 4b_4)^2} - \frac{1}{244 + C_2(5b_7+4b_6+4b_4+40b_1)^2}\right)$$

$$+ B_0\left(\frac{1}{244 + C_2(5b_7 + 4b_6 + 4b_4 + 40b_1)^2}\right) \qquad (2)$$

where $B_m = \frac{C_o}{b_m cI}$, and m = 7, 6, 4, 1 or 0. Note that this equation is linear in the coefficients B_m.

In 15 of the 27 sections, $a_2 = a_3$. By replacing a_3 by a_2 in the expressions for Δ_{j2} and Δ_{j3} in Equation 1a, and adding, we find that, for these sections,

$$\Delta_{j2} + \Delta_{j3} = \frac{C_o}{a_2 cI}\left(\frac{1}{r_j^2 + C_2(a_1D_1)^2} - \frac{1}{r_j^2 + C_2[a_1D_1 + a_2(D_2+D_3)]^2}\right).$$

Also,

$$\Delta_{j4} = \frac{C_o}{a_4 cI}\left(\frac{1}{r_j^2 + C_2\ [a_1D_1 + a_2(D_2 + D_3)]^2} - \frac{1}{r_j^2 + C_2[a_1D_1 + a_2(D_2+D_3) + a_4D_4]^2}\right), \text{ and}$$

$$\Delta_{j5} = \frac{C_o}{a_5 cI}\left(\frac{1}{r_j^2 + C_2[a_1D_1 + a_2(D_2+D_3) + a_4D_4]^2}\right),$$

while the expression for Δ_{j1} remains unchanged.

As an example of how Equation 1a can be applied to a section for which $a_2 = a_3$, consider Section 9 as an example. According to Table 3, the design data for Section 9 are: $D_1 = 5$; $a_1 = b_7$; $D_2 = 4$, $a_2 = b_4$; $D_3 = 4$, $a_3 = b_4$; $D_4 = 40$, $a_4 = b_3$; $a_5 = b_0$. Let j = 2: then $r_j^2 = r_2^2 = 244$. The equation for W_j (or W_2) is:

$$W_2 = B_7\left(\frac{1}{244} - \frac{1}{244 + C_2(5b_7)^2}\right)$$

$$+B_4\left(\frac{1}{244 + C_2(5b_7)^2} - \frac{1}{244 + C_2(5b_7 + 8b_4)^2}\right)$$

$$+B_3\left(\frac{1}{244 + C_2(5b_7 + 8b_4)^2} - \frac{1}{244 + C_2(5b_7 + 8b_4 + 40b_3)^2}\right)$$

$$+B_o\left(\frac{1}{244 + C_2(5b_7 + 8b_4 + 40b_3)^2}\right) \qquad (3)$$

where $B_m = \frac{C_o}{b_m^{\ cI}}$ as before, and m = 7, 4, 3 or 0. This equation, like Equation 2, is linear in the coefficients B_m.

By utilizing the data in Table 3 there can be formed 5 equations like Equations 2 or 3 for each of the 27 test sections, or a total of 135 equations. If trial values are given to the 8 strength coefficients b_m, and to the constant C_2, there results a set of 135 linear equations in the eight coefficients, B_m. From these 135 linear equations, values of the coefficients, B_m, can be estimated by least-squares regression, and the associated error (root-mean-square residual in W_j) can be calculated. We shall refer hereafter to this regression analysis, in which the B_m are evaluated from trial values of C_2 and the b_m, as Regression A.

6.3 Regression B

Once a set of the coefficients B_m has been found, a set of eight linear equations in the constants C_o and C_1 can be written for log B_m in the following form:

$$\log B_m = \log C_o - C_1 \log b_m \tag{4}$$

where m = 0, 1, 2, . . ., 7.

From the eight equations like Equation 4, estimates of log C_o and C_1 can be made, again by least-squares regression. We shall refer hereafter to this regression, in which C_o and C_1 are evaluated, as Regression B.

6.4 Selection of Starting Values

The first step in utilizing the process described above was the selection of starting values for C_2 and the stiffness coefficients, b_m. It was initially assumed that the stiffness coefficients were proportional to the velocity of propagation of compressional waves through the materials in situ. These velocities had been measured during construction of the test facility, and are given in the last column of Table 2 (See Reference 4 for a description of the measurement technique employed). The initial values assigned were equal to the measured wave velocity (feet/second) x 10^{-4}. Values of wave velocity were not available for the foundation material and asphaltic concrete: thus the initial values of b_o and b_7 had to be estimated by other means.

Following selection of initial values of the b_m, a series of values were assigned to C_2 and Regression A was performed for each assigned value of C_2. The value resulting in the least prediction error (root-mean-square residual in W_j) was found to be approximately 6.25. The value of 6.25 was then assigned to C_2, and this value was held fixed throughout the subsequent analysis work.

6.5 The Iteration Procedure

A converging iteration procedure was then followed as indicated below:

Step 1: With C_2 permanently fixed at 6.25, values were assigned to the b_m and Regression A was performed.

Step 2: Regression B was performed.

Step 3: The error, e_m, in each b_m, was computed from the equation:

$$e_m = \underline{\log B_m} - [\underline{\log C_o} - \underline{C_1} \underline{\log b_m}] \qquad (5)$$

wherein the underscored quantities had been evaluated in Steps 1 and/or 2.

Step 4: The following equation was then formed for each value of m:

$$0.5\ \underline{e_m} = \underline{\log B_m} - [\underline{\log C_o} - \underline{C_1} \log b_m]. \qquad (6)$$

wherein the underscored quantities were given their previously calculated values. This equation was then solved for b_m, and the value so obtained was taken as a better estimate of b_m than the value previously assigned in Step 1. Thus at the end of each iteration Step 4 resulted in a new set of starting values for use in Step 1 of a new iteration.

The iteration procedure (Steps 1 through 4) described above was found to be convergent in that the root-mean-square residual in log B_m steadily became smaller with successive iterations, until a lower bound was reached after which further iterations did not produce lesser values of this residual. Furthermore, after each iteration it was discovered that the prediction error of Regression A--that is, the root-mean-square residual in W_j--was reduced below its previous value, until it, too, reached a lower bound at the same time as the root-mean-square residual in log B_m

determined in Regression B. This tendency of both errors to reduce simultaneously was taken as partial evidence that the model represented the physical phenomenon with an acceptable degree of accuracy.

Final values of the constants C_o, C_1, C_2, and of the stiffness coefficients for the materials in the test facility are given in Table 4.

Before concluding the discussion of the analysis of deflection data it should be mentioned that it was discovered early in the analysis work that the deflections measured on Section 1 were not consistent with data taken on the remaining sections. The reasons why these deflections were extraordinarily high is unknown, but they were so "out-of-line" that they were excluded from consideration in the analysis.

TABLE 4: VALUES OF CONSTANTS AND STIFFNESS COEFFICIENTS FOUND FROM ANALYSIS OF TEST FACILITY DEFLECTION DATA

Symbol	Material	Value
C_o	---	.8911
C_1	---	4.5029
C_2	---	6.2500
b_o	Natural Clay Foundation	.1980
b_1	Compacted Clay Embankment	.2709
b_2	Sandy Clay Embankment	.3293
b_3	Sandy Gravel Embankment	.3988
b_4	Cr. Limestone Base or Subbase	.4716
b_5	Cr. Limestone + Lime, Base or Subbase	.5159
b_6	Cr. Limestone + Cement, Base or Subbase	.7902
b_7	Asphaltic Concrete Surfacing	.5222

7. PREDICTION ERRORS

Table 5 lists the relavent design data for all 27 test sections included in the test facility, and contrasts the observed deflections with those predicted from the model when the values given in Table 4 were assigned to the constants and stiffness coefficients. In the last column are shown the individual prediction errors for each Dynaflect sensor. As the reader may see by scanning this column, the errors are generally small compared to the observed values, except in the case of Section 1, the observed data from which, as was mentioned in the last chapter, were inconsistent with the remaining data, and were therefore excluded from the analysis.

In Figure 7 is a plot of the predicted deflections versus the observed deflections. The squared correlation ceofficient between the two variables plotted in the figure was 0.97; that is, 97% of the total variance of the observed values was explained by the model. The root-mean- square residual was .0557 mils, equivalent to 12.2% of the mean value of the deflections. The coefficients of variation of individual sensors ranged from a low of 10.8% for Sensor No. 5 to a high of 13.2% for Sensor No. 4, the overall coefficient of variation being 12.2% as previously mentioned.

When consideration is given to the fact that the tacit assumption was made in the construction of the model, and in the analysis of the data, that a given material--wherever it occurred in the test facility--had an unvarying stiffness coefficient, it is easy to understand how

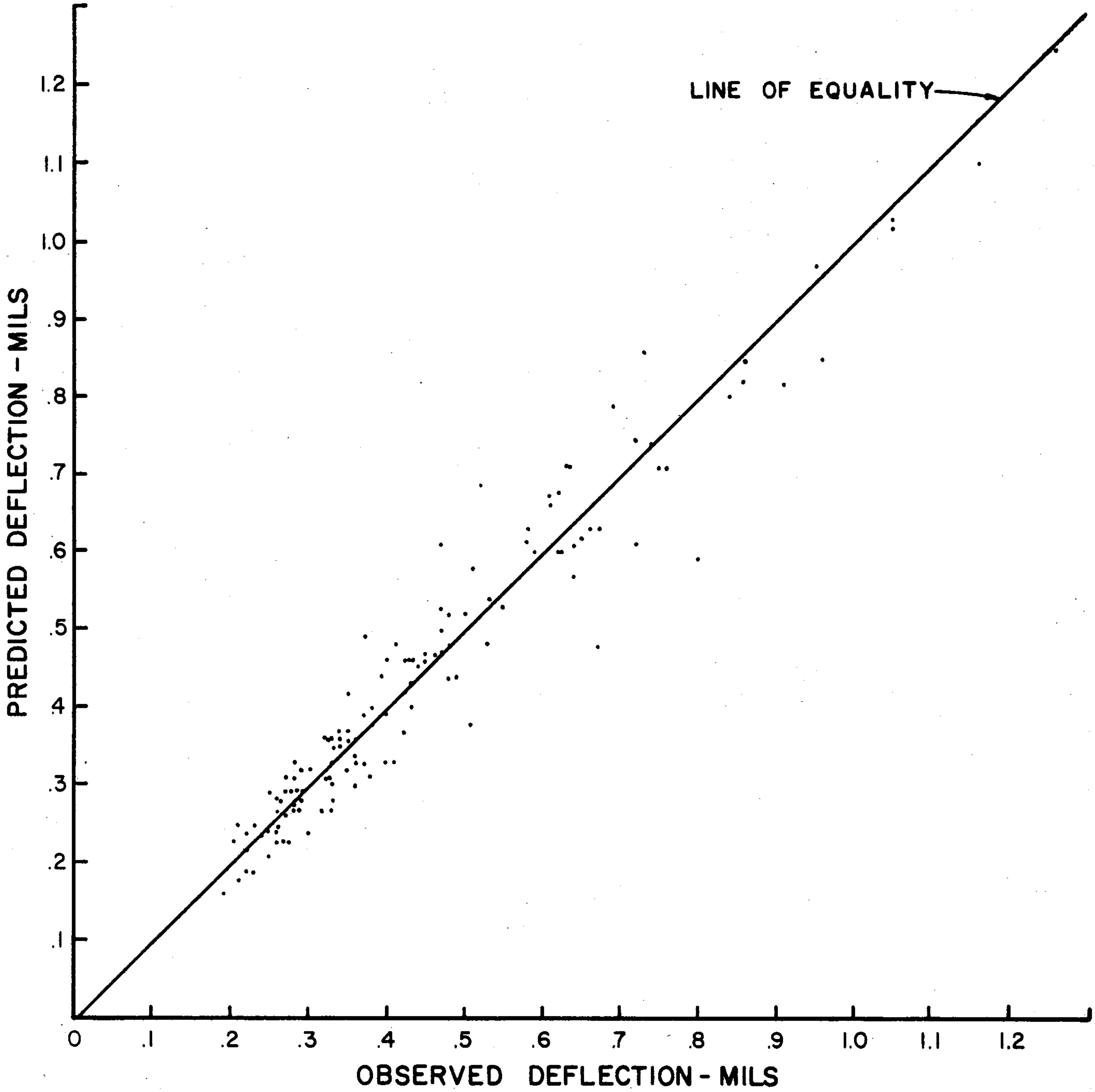

FIGURE 7: Plot of predicted versus observed deflections.

TABLE 5

DEFLECTION COEFFICIENTS AND PREDICTION ERRORS

A&M TEST FACILITY

1966 DATA

SECTION 1

LAYER	MATERIAL	COEFFICIENT	THICKNESS	SENSOR NO.	DEFLECTION (MILS) OBS.	PRED.	ERROR
SURFACE	AC	0.52216	5.0	1	1.92	1.21	0.71
BASE	LS+C	0.79022	4.0	2	1.49	0.97	0.52
SUBBASE	LS	0.47157	4.0	3	1.01	0.66	0.35
EMBANK.	CLAY	0.27087	40.0	4	0.60	0.46	0.14
FOUND.	CLAY	0.19804	999.9	5	0.36	0.33	0.03

SECTION 2

LAYER	MATERIAL	COEFFICIENT	THICKNESS	SENSOR NO.	DEFLECTION (MILS) OBS.	PRED.	ERROR
SURFACE	AC	0.52216	1.0	1	0.52	0.69	-0.17
BASE	LS+C	0.79022	12.0	2	0.47	0.61	-0.14
SUBBASE	LS	0.47157	4.0	3	0.41	0.48	-0.07
EMBANK.	CLAY	0.27087	36.0	4	0.34	0.37	-0.03
FOUND.	CLAY	0.19804	999.9	5	0.29	0.28	0.00

SECTION 3

LAYER	MATERIAL	COEFFICIENT	THICKNESS	SENSOR NO.	DEFLECTION (MILS) OBS.	PRED.	ERROR
SURFACE	AC	0.52216	1.0	1	1.05	1.03	0.02
BASE	LS+C	0.79022	4.0	2	0.86	0.85	0.01
SUBBASE	LS	0.47157	12.0	3	0.58	0.61	-0.03
EMBANK.	CLAY	0.27087	36.0	4	0.39	0.44	-0.05
FOUND.	CLAY	0.19804	999.9	5	0.29	0.32	-0.03

TABLE 5 (Continued)

SECTION 4

LAYER	MATERIAL	COEFFICIENT	THICKNESS	SENSOR NO.	DEFLECTION (MILS) OBS.	PRED.	ERROR
SURFACE	AC	0.52216	5.0	1	0.37	0.49	-0.12
BASE	LS+C	0.79022	12.0	2	0.35	0.42	-0.07
SUBBASE	LS	0.47157	12.0	3	0.32	0.36	-0.04
EMBANK.	CLAY	0.27087	24.0	4	0.28	0.29	-0.01
FOUND.	CLAY	0.19804	999.9	5	0.25	0.24	0.01

SECTION 5

LAYER	MATERIAL	COEFFICIENT	THICKNESS	SENSOR NO.	DEFLECTION (MILS) OBS.	PRED.	ERROR
SURFACE	AC	0.52216	5.0	1	1.26	1.25	0.01
BASE	LS	0.47157	4.0	2	0.95	0.97	-0.02
SUBBASE	LS+C	0.79022	4.0	3	0.61	0.66	-0.05
EMBANK.	CLAY	0.27087	40.0	4	0.40	0.46	-0.06
FOUND.	CLAY	0.19804	999.9	5	0.28	0.33	-0.05

SECTION 6

LAYER	MATERIAL	COEFFICIENT	THICKNESS	SENSOR NO.	DEFLECTION (MILS) OBS.	PRED.	ERROR
SURFACE	AC	0.52216	1.0	1	1.16	1.10	0.06
BASE	LS	0.47157	12.0	2	0.96	0.85	0.11
SUBBASE	LS+C	0.79022	4.0	3	0.72	0.61	0.11
EMBANK.	CLAY	0.27087	36.0	4	0.49	0.44	0.05
FOUND.	CLAY	0.19804	999.9	5	0.35	0.32	0.03

SECTION 7

LAYER	MATERIAL	COEFFICIENT	THICKNESS	SENSOR NO.	DEFLECTION (MILS) OBS.	PRED.	ERROR
SURFACE	AC	0.52216	1.0	1	0.74	0.74	0.00
BASE	LS	0.47157	4.0	2	0.65	0.62	0.03
SUBBASE	LS+C	0.79022	12.0	3	0.53	0.48	0.05
EMBANK.	CLAY	0.27087	36.0	4	0.42	0.37	0.05
FOUND.	CLAY	0.19804	999.9	5	0.33	0.28	0.05

TABLE 5 (Continued)

SECTION 8

LAYER	MATERIAL	COEFFICIENT	THICKNESS	SENSOR NO.	DEFLECTION (MILS) OBS.	PRED.	ERROR
SURFACE	AC	0.52216	5.0	1	0.62	0.60	0.02
BASE	LS	0.47157	12.0	2	0.43	0.46	-0.03
SUBBASE	LS+C	0.79022	12.0	3	0.33	0.36	-0.03
EMBANK.	CLAY	0.27087	24.0	4	0.28	0.29	-0.01
FOUND.	CLAY	0.19804	999.9	5	0.24	0.24	0.00

SECTION 9

LAYER	MATERIAL	COEFFICIENT	THICKNESS	SENSOR NO.	DEFLECTION (MILS) OBS.	PRED.	ERROR
SURFACE	AC	0.52216	5.0	1	0.75	0.71	0.04
BASE	LS	0.47157	4.0	2	0.55	0.53	0.02
SUBBASE	LS	0.47157	4.0	3	0.38	0.40	-0.02
EMBANK.	GRAV	0.39880	40.0	4	0.27	0.31	-0.04
FOUND.	CLAY	0.19804	999.9	5	0.21	0.25	-0.04

SECTION 10

LAYER	MATERIAL	COEFFICIENT	THICKNESS	SENSOR NO.	DEFLECTION (MILS) OBS.	PRED.	ERROR
SURFACE	AC	0.52216	1.0	1	0.63	0.71	-0.08
BASE	LS	0.47157	12.0	2	0.50	0.52	-0.02
SUBBASE	LS	0.47157	4.0	3	0.40	0.39	0.00
EMBANK.	GRAV	0.39880	36.0	4	0.32	0.31	0.00
FOUND.	CLAY	0.19804	999.9	5	0.26	0.25	0.01

SECTION 11

LAYER	MATERIAL	COEFFICIENT	THICKNESS	SENSOR NO.	DEFLECTION (MILS) OBS.	PRED.	ERROR
SURFACE	AC	0.52216	1.0	1	0.63	0.71	-0.08
BASE	LS	0.47157	4.0	2	0.48	0.52	-0.04
SUBBASE	LS	0.47157	12.0	3	0.37	0.39	-0.02
EMBANK.	GRAV	0.39880	36.0	4	0.28	0.31	-0.03
FOUND.	CLAY	0.19804	999.9	5	0.23	0.25	-0.02

TABLE 5 (Continued)

SECTION 12

LAYER	MATERIAL	COEFFICIENT	THICKNESS	SENSOR NO.	DEFLECTION (MILS) OBS.	PRED.	ERROR
SURFACE	AC	0.52216	5.0	1	0.64	0.61	0.03
BASE	LS	0.47157	12.0	2	0.45	0.46	-0.01
SUBBASE	LS	0.47157	12.0	3	0.32	0.36	-0.04
EMBANK.	GRAV	0.39880	24.0	4	0.25	0.29	-0.04
FOUND.	CLAY	0.19804	999.9	5	0.20	0.23	-0.03

SECTION 13

LAYER	MATERIAL	COEFFICIENT	THICKNESS	SENSOR NO.	DEFLECTION (MILS) OBS.	PRED.	ERROR
SURFACE	AC	0.52216	5.0	1	0.47	0.47	-0.00
BASE	LS+C	0.79022	4.0	2	0.43	0.40	0.03
SUBBASE	LS+C	0.79022	4.0	3	0.36	0.33	0.03
EMBANK.	GRAV	0.39880	40.0	4	0.28	0.27	0.01
FOUND.	CLAY	0.19804	999.9	5	0.22	0.22	0.00

SECTION 14

LAYER	MATERIAL	COEFFICIENT	THICKNESS	SENSOR NO.	DEFLECTION (MILS) OBS.	PRED.	ERROR
SURFACE	AC	0.52216	1.0	1	0.40	0.33	0.07
BASE	LS+C	0.79022	12.0	2	0.37	0.30	0.07
SUBBASE	LS+C	0.79022	4.0	3	0.33	0.27	0.06
EMBANK.	GRAV	0.39880	36.0	4	0.27	0.23	0.04
FOUND.	CLAY	0.19804	999.9	5	0.23	0.19	0.04

SECTION 15

LAYER	MATERIAL	COEFFICIENT	THICKNESS	SENSOR NO.	DEFLECTION (MILS) OBS.	PRED.	ERROR
SURFACE	AC	0.52216	1.0	1	0.41	0.33	0.08
BASE	LS+C	0.79022	4.0	2	0.36	0.30	0.06
SUBBASE	LS+C	0.79022	12.0	3	0.32	0.27	0.05
EMBANK.	GRAV	0.39880	36.0	4	0.27	0.23	0.04
FOUND.	CLAY	0.19804	999.9	5	0.22	0.19	0.03

TABLE 5 (Continued)

SECTION 16

LAYER	MATERIAL	COEFFICIENT	THICKNESS	SENSOR NO.	DEFLECTION (MILS) OBS.	PRED.	ERROR
SURFACE	AC	0.52216	5.0	1	0.29	0.29	0.00
BASE	LS+C	0.79022	12.0	2	0.26	0.23	0.03
SUBBASE	LS+C	0.79022	12.0	3	0.25	0.21	0.04
EMBANK.	GRAV	0.39880	24.0	4	0.21	0.18	0.03
FOUND.	CLAY	0.19804	999.9	5	0.19	0.16	0.03

SECTION 17

LAYER	MATERIAL	COEFFICIENT	THICKNESS	SENSOR NO.	DEFLECTION (MILS) OBS.	PRED.	ERROR
SURFACE	AC	0.52216	3.0	1	0.72	0.75	-0.03
BASE	LS+L	0.51587	8.0	2	0.59	0.60	-0.00
SUBBASE	LS+L	0.51587	8.0	3	0.44	0.46	-0.02
EMBANK.	SC	0.32934	34.0	4	0.33	0.35	-0.02
FOUND.	CLAY	0.19804	999.9	5	0.26	0.27	-0.01

SECTION 18

LAYER	MATERIAL	COEFFICIENT	THICKNESS	SENSOR NO.	DEFLECTION (MILS) OBS.	PRED.	ERROR
SURFACE	AC	0.52216	1.0	1	0.84	0.80	0.04
BASE	LS+L	0.51587	8.0	2	0.66	0.63	0.03
SUBBASE	LS+L	0.51587	8.0	3	0.48	0.48	0.00
EMBANK.	SC	0.32934	36.0	4	0.36	0.36	-0.00
FOUND.	CLAY	0.19804	999.9	5	0.28	0.28	0.00

SECTION 19

LAYER	MATERIAL	COEFFICIENT	THICKNESS	SENSOR NO.	DEFLECTION (MILS) OBS.	PRED.	ERROR
SURFACE	AC	0.52216	5.0	1	0.76	0.71	0.05
BASE	LS+L	0.51587	8.0	2	0.64	0.57	0.07
SUBBASE	LS+L	0.51587	8.0	3	0.48	0.44	0.04
EMBANK.	SC	0.32934	32.0	4	0.36	0.34	0.02
FOUND.	CLAY	0.19804	999.9	5	0.28	0.27	0.01

TABLE 5 (Continued)

SECTION 20

LAYER	MATERIAL	COEFFICIENT	THICKNESS	SENSOR NO.	DEFLECTION (MILS) OBS.	PRED.	ERROR
SURFACE	AC	0.52216	3.0	1	0.73	0.86	-0.13
BASE	LS+L	0.51587	4.0	2	0.61	0.67	-0.06
SUBBASE	LS+L	0.51587	8.0	3	0.47	0.50	-0.03
EMBANK.	SC	0.32934	38.0	4	0.35	0.37	-0.02
FOUND.	CLAY	0.19804	999.9	5	0.27	0.29	-0.02

SECTION 21

LAYER	MATERIAL	COEFFICIENT	THICKNESS	SENSOR NO.	DEFLECTION (MILS) OBS.	PRED.	ERROR
SURFACE	AC	0.52216	3.0	1	0.62	0.68	-0.06
BASE	LS+L	0.51587	12.0	2	0.53	0.54	-0.01
SUBBASE	LS+L	0.51587	8.0	3	0.42	0.42	-0.00
EMBANK.	SC	0.32934	30.0	4	0.33	0.33	-0.00
FOUND.	CLAY	0.19804	999.9	5	0.27	0.26	0.00

SECTION 24

LAYER	MATERIAL	COEFFICIENT	THICKNESS	SENSOR NO.	DEFLECTION (MILS) OBS.	PRED.	ERROR
SURFACE	AC	0.52216	3.0	1	0.91	0.82	0.09
BASE	LS	0.47157	8.0	2	0.67	0.63	0.04
SUBBASE	LS+L	0.51587	8.0	3	0.46	0.47	-0.01
EMBANK.	SC	0.32934	34.0	4	0.34	0.36	-0.02
FOUND.	CLAY	0.19804	999.9	5	0.26	0.28	-0.02

SECTION 25

LAYER	MATERIAL	COEFFICIENT	THICKNESS	SENSOR NO.	DEFLECTION (MILS) OBS.	PRED.	ERROR
SURFACE	AC	0.52216	3.0	1	0.47	0.53	-0.06
BASE	LS+C	0.79022	8.0	2	0.43	0.46	-0.03
SUBBASE	LS+L	0.51587	8.0	3	0.38	0.38	-0.00
EMBANK.	SC	0.32934	34.0	4	0.32	0.31	0.01
FOUND.	CLAY	0.19804	999.9	5	0.26	0.24	0.02

TABLE 5 (Continued)

SECTION 26

LAYER	MATERIAL	COEFFICIENT	THICKNESS	SENSOR NO.	DEFLECTION (MILS) OBS.	PRED.	ERROR
SURFACE	AC	0.52216	3.0	1	0.69	0.79	-0.10
BASE	LS+L	0.51587	8.0	2	0.58	0.63	-0.05
SUBBASE	LS	0.47157	8.0	3	0.45	0.47	-0.02
EMBANK.	SC	0.32934	34.0	4	0.34	0.36	-0.02
FOUND.	CLAY	0.19804	999.9	5	0.26	0.28	-0.02

SECTION 27

LAYER	MATERIAL	COEFFICIENT	THICKNESS	SENSOR NO.	DEFLECTION (MILS) OBS.	PRED.	ERROR
SURFACE	AC	0.52216	3.0	1	0.80	0.59	0.21
BASE	LS+L	0.51587	8.0	2	0.67	0.48	0.19
SUBBASE	LS+C	0.79022	8.0	3	0.51	0.38	0.13
EMBANK.	SC	0.32934	34.0	4	0.38	0.31	0.07
FOUND.	CLAY	0.19804	999.9	5	0.30	0.24	0.06

SECTION 28

LAYER	MATERIAL	COEFFICIENT	THICKNESS	SENSOR NO.	DEFLECTION (MILS) OBS.	PRED.	ERROR
SURFACE	AC	0.52216	3.0	1	1.05	1.02	0.03
BASE	LS+L	0.51587	8.0	2	0.86	0.82	0.04
SUBBASE	LS+L	0.51587	8.0	3	0.62	0.60	0.02
EMBANK.	CLAY	0.27087	34.0	4	0.43	0.43	-0.00
FOUND.	CLAY	0.19804	999.9	5	0.30	0.32	-0.02

SECTION 29

LAYER	MATERIAL	COEFFICIENT	THICKNESS	SENSOR NO.	DEFLECTION (MILS) OBS.	PRED.	ERROR
SURFACE	AC	0.52216	3.0	1	0.51	0.58	-0.07
BASE	LS+L	0.51587	8.0	2	0.43	0.46	-0.03
SUBBASE	LS+L	0.51587	8.0	3	0.35	0.36	-0.01
EMBANK.	GRAV	0.39880	34.0	4	0.28	0.29	-0.01
FOUND.	CLAY	0.19804	999.9	5	0.22	0.24	-0.02

ROOT MEAN SQUARE RESIDUAL 0.12139240E 00 errors of 10% or greater in predicted deflections could arise. The writers therefore believe that errors of this magnitude must be expected, and that the model represents the deflection phenomenon with acceptable accuracy.

8. STIFFNESS COEFFICIENTS OF EXISTING HIGHWAYS

The following question arises: if a set of Dynaflect measurements--W_1, W_2, W_3, W_4 and W_5--are taken on an existing highway for which the layer thicknesses are known, can the stiffness coefficients--a_1, a_2, etc.--be computed from the deflection equation presented herein?

Experience dictates an answer of no to this question, except in the special case of a simple structure consisting of a relatively thin surfacing layer--say less than two inches--on a base with no sub-base layers between base and subgrade. In this special case the surfacing and base layers can be considered one material, with a thickness of D_1 and stiffness of a_1, resting on a semi-infinite foundation with a stiffness, a_2.

Consider the deflections W_1 and W_2. The equations for these deflections are, according to Equation 1-

$$W_1 = \frac{C_o}{a_1^{C1}}\left(\frac{1}{r_1^2} - \frac{1}{r_1^2 + 6.25\ (a_1D_1)^2}\right) + \frac{C_o}{a_2^{C1}}\left(\frac{1}{r_1^2+6.25\ (a_1D_1)^2}\right) \qquad (7)$$

$$W_2 = \frac{C_o}{a_1^{C1}}\left(\frac{1}{r_2^2} - \frac{1}{r_2^2 + 6.25\ (a_1D_1)^2}\right) + \frac{C_o}{a_2^{C1}}\left(\frac{1}{r_2^2+6.25(a_1D_1)^2}\right) \qquad (8)$$

where C_o, C_1, r_1^2 and r_2^2 are known (see Table 4 and Chapter 5).

By eliminating a_2 between these two equations, the following equation in a_1 can be formed:

$$\frac{W_1 - \dfrac{C_o}{a_1^{C1}}\left(\dfrac{1}{r_1^2} - \dfrac{1}{r_1^2 + 6.25\ (a_1D_1)^2}\right)}{W_2 - \dfrac{C_o}{a_1^{C1}}\left(\dfrac{1}{r_2^2} - \dfrac{1}{r_2^2 + 6.25\ (a_1D_1)^2}\right)} - \frac{r_2^2 + 6.25\ (a_1D_1)^2}{r_1^2 + 6.25\ (a_1D_1)^2} = 0 \qquad (9)$$

In equation 9 all quantities except a_1 are known. The value of a_1 can be found by iteration (trial and error). With a_1 known, a_2 can be found from either Equation 7 or Equation 8, since a_2 can be isolated in either of those equations.

The above procedure was used in estimating the base and foundation coefficients given in Tables 4 and 5 of Research Report 32-11.

In theory any pair of the deflections W_j can be used to find a_1 and a_2, and the values found from any pair should equal those found from any other pair. In practice it has been discovered that this rule does not generally hold--the values found by using W_1 and W_2, for example, are, in fact, not precisely the same as those found from W_1 and W_5. The difference is ascribed to experimental error, including the error in assuming that a simple two-layer structure of the type envisioned actually can exist in the case of a real pavement and its foundation. The difference can also be ascribed to imperfections in the mathematical model.

Means for improving the accuracy of stiffness estimates from Dynaflect data using the model presented herein are still under investigation. In addition, current research in Research Project 136 has as its prime objective the development of a more perfect model of the deflection phenomenon.

9. CONCLUSIONS

While the model presented in this report proved to be very efficient when tested against the deflection data, these writers believe a still better model will result from current research. Meanwhile, the present model appears to be sufficiently accurate to merit its use in the design procedure described in Research Report 32-11.

LIST OF REFERENCES

1. Scrivner, F. H.; Moore, W. M.; McFarland, W. F., and Carey, G. R. "A Systems Approach To The Flexible Pavement Design Problem," Research Report 32-11, Texas Transportation Institute, Texas A&M University, College Station, Texas, 1968 (in press).

2. Scrivner, F. H.; Swift, Gilbert; and Moore, W. M. "A New Research Tool for Measuring Pavement Deflection," Highway Research Record No. 129, Highway Research Board, Washington, D. C., pp. 1-11, 1966.

3. Pace, George M. "Evaluation of the Dynaflect for the Non-Destructive Testing of Portland Cement Concrete Pavements," Technical Report No. 4-61, Department of the Army, Ohio Division Laboratories, Corps of Engineers, Cincinnait, Ohio, 1967.

4. Scrivner, F. H. and Moore, W. M. "Evaluation of the Stiffness of Individual Layers in a Specially Designed Pavement Facility from Surface Deflections," Research Report 32-8, Texas Transportation Institute, Texas A&M University, College Station, Texas, 1966.

APPENDIX A: CONSTRUCTION OF MODEL OF PAVEMENT DEFLECTION

Figure 8 defines the symbols used to describe the position of an element in the ith layer of a system of n + 1 layers loaded vertically at the origin of coordinates. Displacements are symmetrical about the z-axis. Other definitions follow:

ε_z = vertical strain at any point in the system.

w = vertical displacement at any point in the system.

w_1, w_2 = vertical displacements at the points r, z_1 and r, z_2, located in the upper and lower boundaires, respectively, of the ith layer.

Since $\varepsilon_z = \frac{\partial w}{\partial z}$, it follows that the displacement, w, is given by the equation

$$w = \int_z^{\infty} \varepsilon_z dz$$

where the limit z is the coordinate of the point with displacement w.

It follows that

$$w_1 = \int_{z_1}^{\infty} \varepsilon_z dz .$$

The preceeding integral may be separated into two parts as indicated below:

$$w_1 = \int_{z_1}^{z_2} \varepsilon_z dz + \int_{z_2}^{\infty} \varepsilon_z dz.$$

The second of the two integrals above is obviously w_2. Thus,

$$w_1 = \int_{z_1}^{z_2} \varepsilon_z dz + w_2, \text{ or}$$

$$w_1 - w_2 = \int_{z_1}^{z_2} \varepsilon_z dz.$$

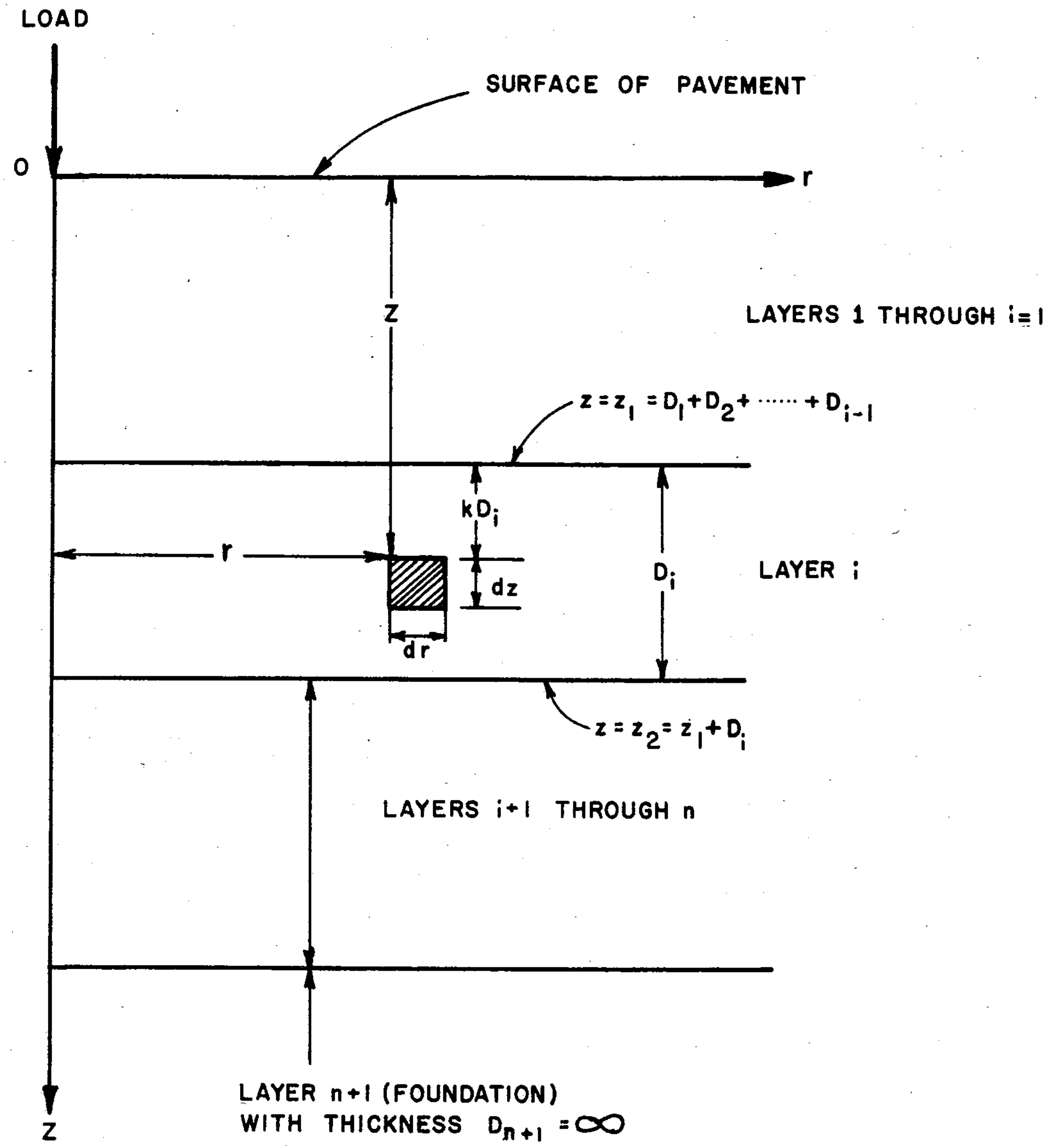

FIGURE 8: Symbols used to define the position of an element in the i^{th} layer of a system of n + 1 layers.

The quantity $w_1 - w_2$ is the change in thickness of the ith layer due to the application of the load. This quantity we represent by the symbol, Δ_i. Then

$$\Delta_i = \int_{z_1}^{z_2} \varepsilon_z dz. \tag{1}$$

The deflection, w_s, at a point in the surface is found by summing all the Δ_i, i.e.

$$w_s = \sum_{i=1}^{n+1} \Delta_i \tag{2}$$

In order to calculate w_s, the expression for ε_z in the ith layer must be known. The expression for ε_z provided by elasticity theory is too complex for present purposes. Therefore, a simpler expression was developed in conjunction with a transformation of the coordinate, z (See Figure 9). The coordinate z of an element in the ith layer is transformed to the coordinate m, which is computed from the equation

$$m = C\ (a_1D_1 + a_2D_2 + \ldots + a_{i-1}D_{i-1} + ka_iD_i) \tag{3}$$

where C is a constant; the coefficients a_1, a_2, etc. are taken to be measures of the stiffness of the material composing the first, second, etc. layers of the system; and k is a variable whose value is restricted to the interval 0 to 1.

As indicated in Figure 8, the expression for z corresponding to the preceeding equation for m is

$$a = D_1 + D_2 + \ldots + D_{i-1} + kD_i \tag{4}$$

By comparing the expressions for m and z it can be seen that the value of m is dependent on both the thickness and the stiffness of the materials

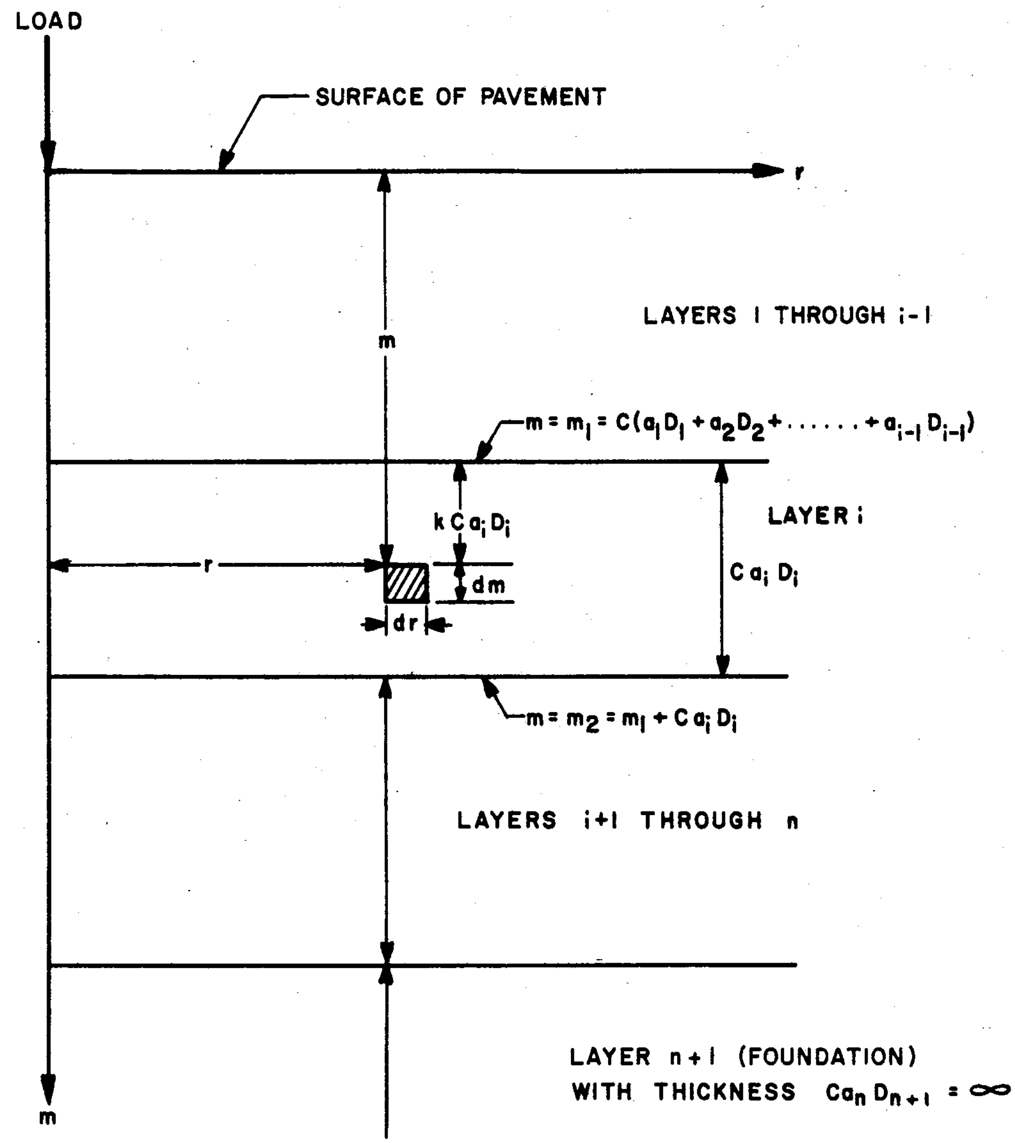

FIGURE 9: Symbols used to define the position of the element in the transformed coordinate system.

located above the element while the value of z depends, of course, only on the thickness of those materials.

From Equation 4 it is seen that

$$dz = D_i dk$$

and, from Equation 3, that

$$dm = Ca_i D_i dk.$$

It follows from these two equations that

$$dz = \frac{dm}{Ca_i} \quad .$$

We find the transform of Equation 1 by substituting dm/Ca_i for dz in Equation 1, with the following result:

$$\Delta_i = \frac{1}{Ca_i} \int_{m_1}^{m_2} \varepsilon_z dm \qquad (5)$$

The expression for the vertical strain of an element in the ith layer, finally adopted after several expressions had been tested against the deflection data gathered on the test facility, was the following:

$$\varepsilon_z = \frac{B_i m}{(r^2+m^2)^2} \qquad (6)$$

where B_i is assumed to be some function of a_i.

It can be seen from Equation 6 that increasing either the thickness <u>or the stiffness</u> of the overlying layers results in a decrease in ε_z. It was to achieve this result that the transformation from z to m was made.

From Equations 5 and 6 it follows that

$$\Delta_i = \frac{B_i}{Ca_i} \int_{m_1}^{m_2} \frac{m\, dm}{(r^2+m^2)^2}$$

By performing the indicated integration we obtain

$$\Delta_i = \frac{B_i}{2}\left(\frac{1}{r^2+m_1{}^2} - \frac{1}{r^2+m_2{}^2}\right) .$$

Finally, we define B_i more definitely by the equation

$$B_i = \frac{2C_o}{a_i^{c1}} ,$$

where C_o and C_1 are constants. The expression for Δ_i then becomes

$$\Delta_i = \frac{C_o}{a_i^{c1}}\left(\frac{1}{r^2 + C^2(a_1D_1 + a_2D_2 + \ldots + a_{i-1}D_{i-1})^2} - \frac{1}{r^2 + C^2(a_1D_1 + a_2D_2 + \ldots + a_iD_i)^2}\right) \qquad (7)$$

This equation can be made to take the form of the equation for Δ_{jk} given in Chapter 5 by first replacing C^2 by C_2, and then making the indicated changes in subscripts.

While the model arrived at as described above proved to be very efficient when tested against the deflection data, these writers believe a better model will eventually be constructed. Meanwhile, the present model appears to be sufficiently accurate to merit its use in the design procedure described in Research Report 32-11.